Chronic Stress Remodels Synapses in an Amygdala Circuit-Specific Manner

Supplemental Information

Supplemental Methods and Materials

Electrophysiological recordings

Electrophysiology recordings were performed as described previously (1). Briefly, the mice aged at 60-70 days were anesthetized with diethyl ether and immediately sacrificed by decapitation. Their brains were quickly removed and placed in ice-cold oxygenated (95% O_2/5% CO_2) artificial cerebrospinal fluid (ACSF) containing (in mM): 124 NaCl, 2.5 KCl, 1 $MgSO_4$, 2.5 $CaCl_2$, 10 glucose, and 26 $NaHCO_3$ and kept there for ~3 minutes. Coronal brain sections containing the amygdala were cut with a tissue slicer (Leica VT 1000S) and maintained at room-temperature for at least 1 hour before recording. Slices were then transferred to a recording chamber continuously superfused with ACSF at a constant rate of about 60 ml/h. Temperature was held at 29±1°C. Pipette solutions contained (in mM) 120 Kgluconate, 5 NaCl, 1 $MgCl_2$, 10 HEPES, and 0.2 EGTA, 2 ATP-Mg and 0.1 GTP-Na. The Kgluconate was replaced by same concentration of CsCl in experiments recording mIPSCs. The pH was adjusted to 7.3 with KOH or CsOH appropriately and osmolarity to 295 Osm with sucrose. The pipette resistance was around 4-7 MΩ. The cells were held at -70mV. A junction potential of ~12 mV was uncorrected.

The BLA→dmPFC and BLA↛dmPFC PNs were differentiated under the fluorescent microscope based on the presence and absence, respectively, of fluorescent RetroBeads in their

soma. To record miniature excitatory postsynaptic currents (mEPSCs), TTX (1 μM), APV (20 μM) and picrotoxin (100 μM) were added. To record miniature inhibitory postsynaptic currents (mIPSCs), TTX, APV (Sigma-Aldrich) and CNQX (Sigma-Aldrich) (20 μM) were added. The evoked EPSCs (eEPSCs) were recorded in the presence of picrotoxin and the bipolar electrodes were placed close to the border between lateral and basal amygdala. For assessing the rate of NMDAR current blockage by MK-801, the recorded neuron was clamped at +40 mV, and the baseline of synaptic responses to 0.1 Hz presynaptic stimulation were recorded for 3 minutes, followed by the bath application of MK-801 (20 μM) for 5 minutes without stimulation. Stimulation at 0.1 Hz was then resumed for 20 minutes. EPSC amplitudes were normalized to the first EPSC and fitted with the single-exponential function to calculate the decay constant (τ). Series resistance (Rs) was in the range of 10-20 MΩ under whole-cell recordings and monitored throughout experiments. If Rs changed more than 20% during recording, the data were not included in analysis. Data were sampled at 10K Hz and filtered at 2K Hz using the patch-clamp amplifier (HEKA EPC 10 USB Double) circuitry. The mEPSCs and mIPSCs were analyzed offline using Minianalysis (Synaptosoft) and the eEPSCs with Origin8.5 (Originlab, Inc.).

Supplementary Figures

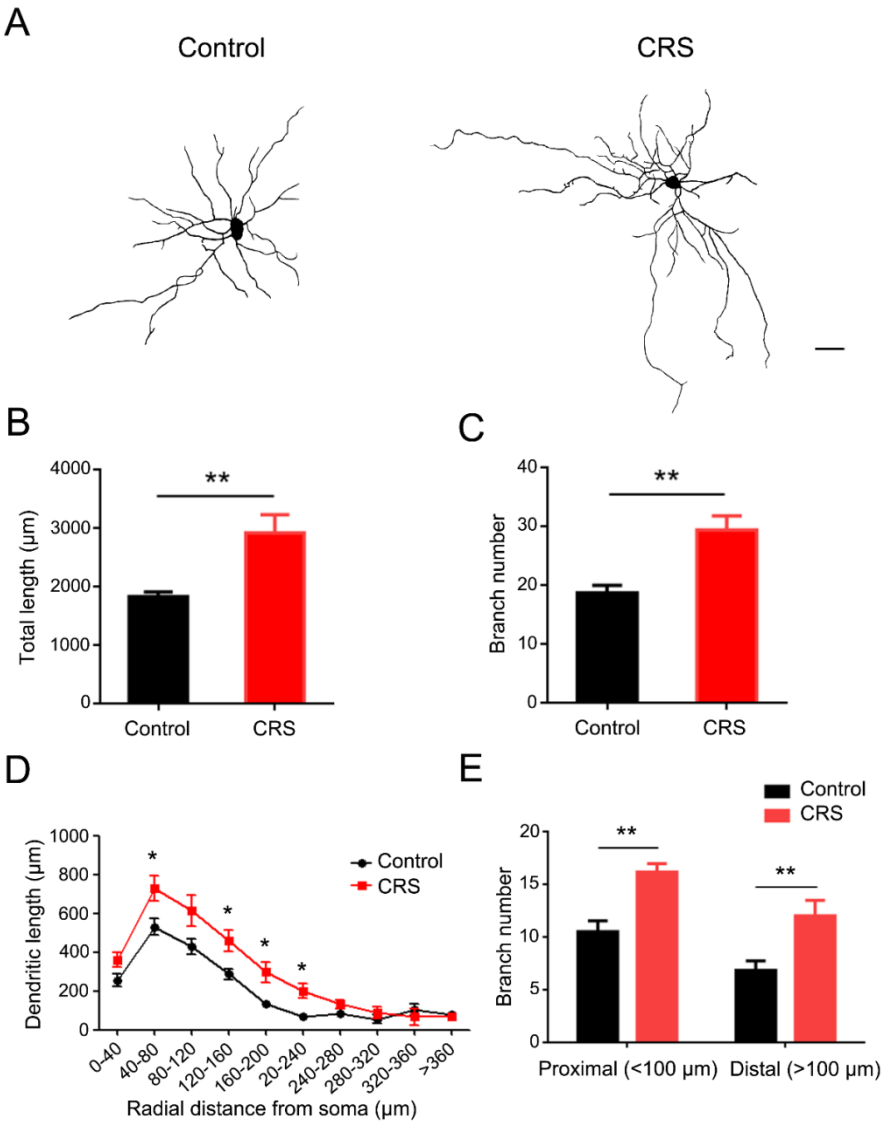

Figure S1. CRS causes dendritic hypertrophy in randomly-selected BLA PNs.

(A) Reconstructed BLA PNs from control and CRS mice. Scale bar: 30 μm.

(B-C) Summary of the total dendritic length (B) and branch number (C) of BLA PNs. n=6 neurons/4 control mice and n=6 neurons/4 CRS mice. t-test, **p<0.01.

(D) Plot of dendritic length as a function of its radical distance from the soma. n=6 neurons/4 controls and n=6 neurons/4 CRS. Distance x CRS two-way ANOVA: Interaction: $F(9,78)=1.20$, $p=0.308$; main effect of distance: $F(9,78)=36.77$, $p<0.001$; main effect of CRS, $F(1,78)=16.38$, $p<0.001$, t-test, *p<0.05.

(E) Summary of the branch number in the proximal and distal dendrites. Distance x CRS two-way ANOVA: Interaction: $F(1,20)=0.05$, $p=0.820$; main effect of distance: $F(1,20)=13.04$, $p=0.002$; main effect of CRS, $F(1,20)=24.94$, $p<0.001$, t-test,**p<0.01.

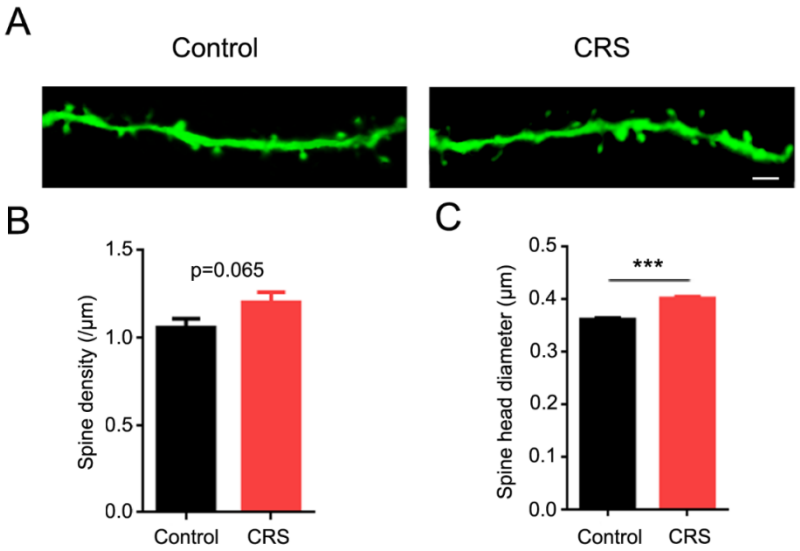

Figure S2. Regulation of CRS on the dendritic spines in randomly-selected BLA PNs.

(A) Representative images showing the dendritic spines of BLA PNs from control and CRS mice. Scale bar: 2 μm.

(B) Summary of the spine density in BLA PNs. n=6 neurons/5 controls and n=7 neurons/5 CRS.

(C) Summary of the spine head size in BLA PNs. n=2285 spines /6 control neurons and n= 2816 spines /7 CRS neurons. t-test, ***p<0.001.

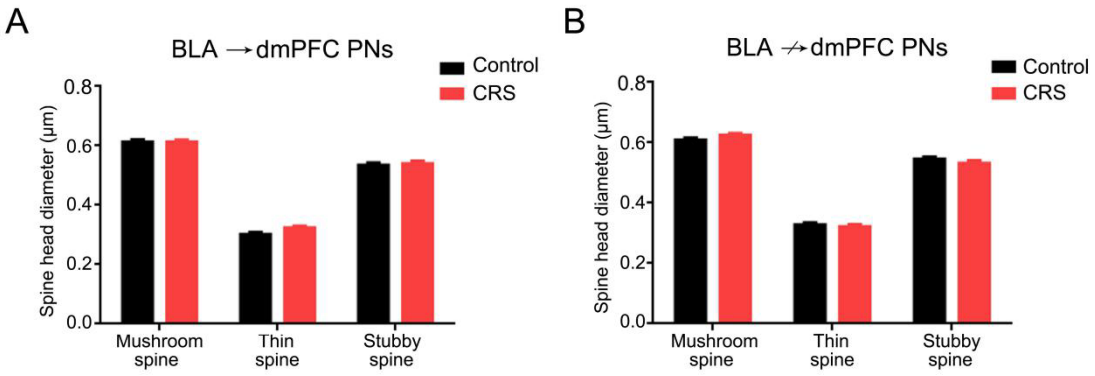

Figure S3. Effect of CRS on the head size of the three spine types in BLA→dmPFC and BLA↛dmPFC PNs.

(A-B) Summary of the head size of the three spine types in BLA→dmPFC (A) and BLA↛dmPFC PNs (B). For BLA→dmPFC PNs: spine type x CRS two-way ANOVA: Interaction: $F(2,8301)=4.337$, $p=0.013$; main effect of spine type: $F(2,8301)=571.69$, $p<0.001$; main effect of CRS: $F(1,8301)=0.145$, $p=0.703$, Control, mushroom, n=426; thin, n=3197; stubby, n=485; CRS mice, mushroom, n=590; thin, n=3306; stubby, n=303; For BLA↛dmPFC PNs: spine type x CRS two-way ANOVA: Interaction: $F(2,8815)=10.591$, $p<0.001$; main effect of spine type: $F(2,8815)=5148.04$, $p<0.001$; main effect of CRS: $F(1,8815)=2.98$, $p=0.329$, Control, mushroom, n=755; thin, n=3919; stubby, n=688; CRS mice, mushroom, n=758; thin, n=2310; stubby, n=391.

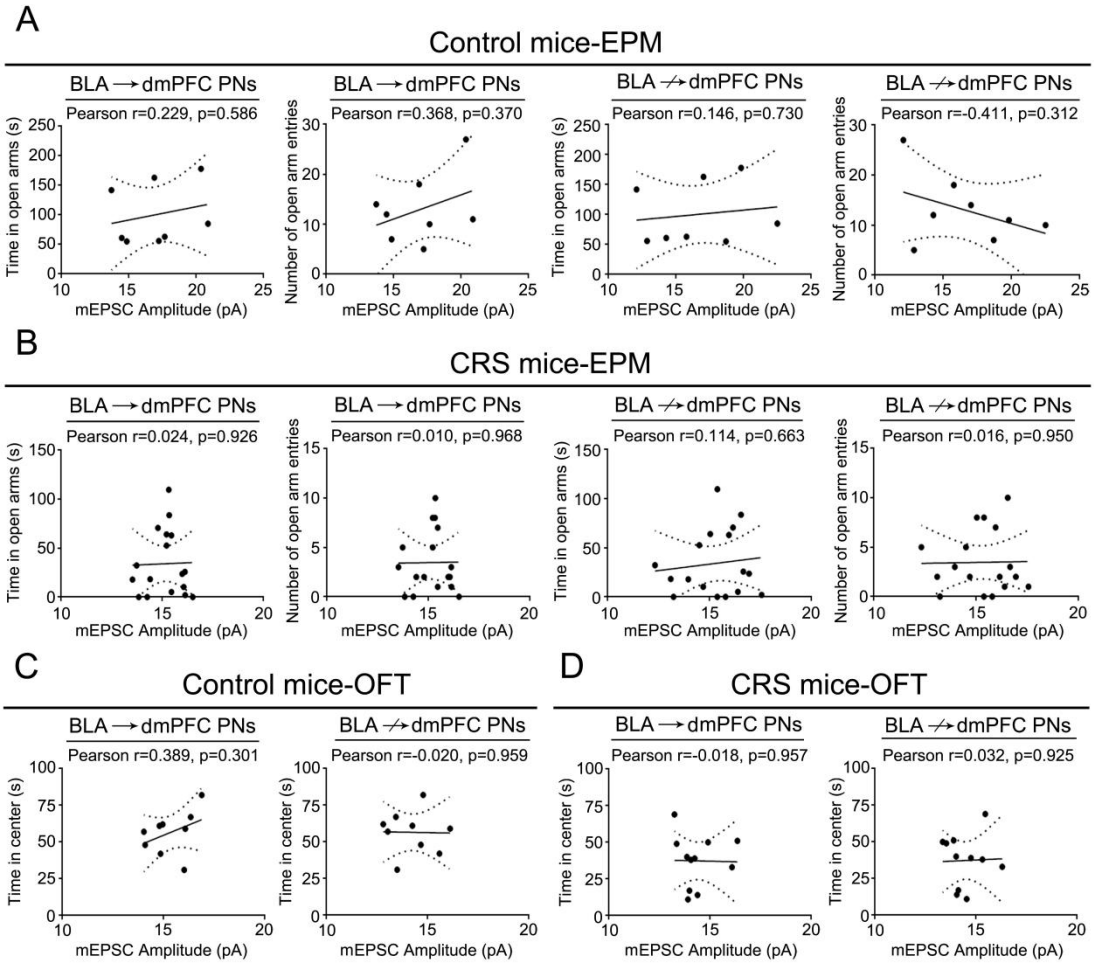

Figure S4. The anxiety-like behavior in control and CRS mice does not correlate with the mEPSCs amplitude in BLA→dmPFC or BLA↛dmPFC PNs.

(A-B) Correlation between the open arm exploration of control (A) and CRS mice (B) in the elevated plus maze (EPM) with the mEPSCs amplitude in BLA→dmPFC and BLA↛dmPFC PNs.

(C-D) Correlation between the center square exploration of control (C) and CRS mice (D) in the open field test (OFT) with the mEPSCs amplitude in BLA→dmPFC and BLA↛dmPFC PNs.

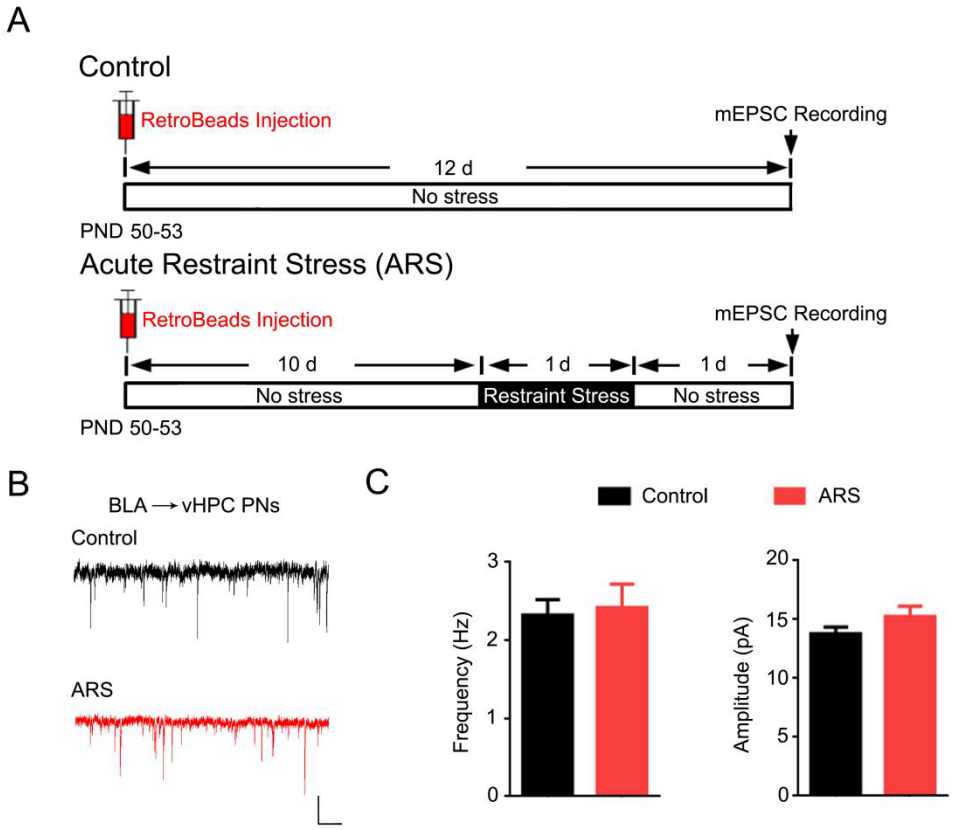

Figure S5. Acute restraint stress does not alter mEPSCs in BLA→vHPC and BLA→NAc PNs.

(A) Schematic showing the experimental design.

(B) Representative traces showing mEPSCs in BLA→vHPV PNs. Scale bar = 1 sec, 10 pA.

(C) Average mEPSC frequency and amplitude in BLA→vHPC PNs. n= 9 neurons/3 controls and n=10 neurons/3 ARS. t test for mEPSCs frequency, p=0.880; for mEPSCs amplitude, p=0.652.

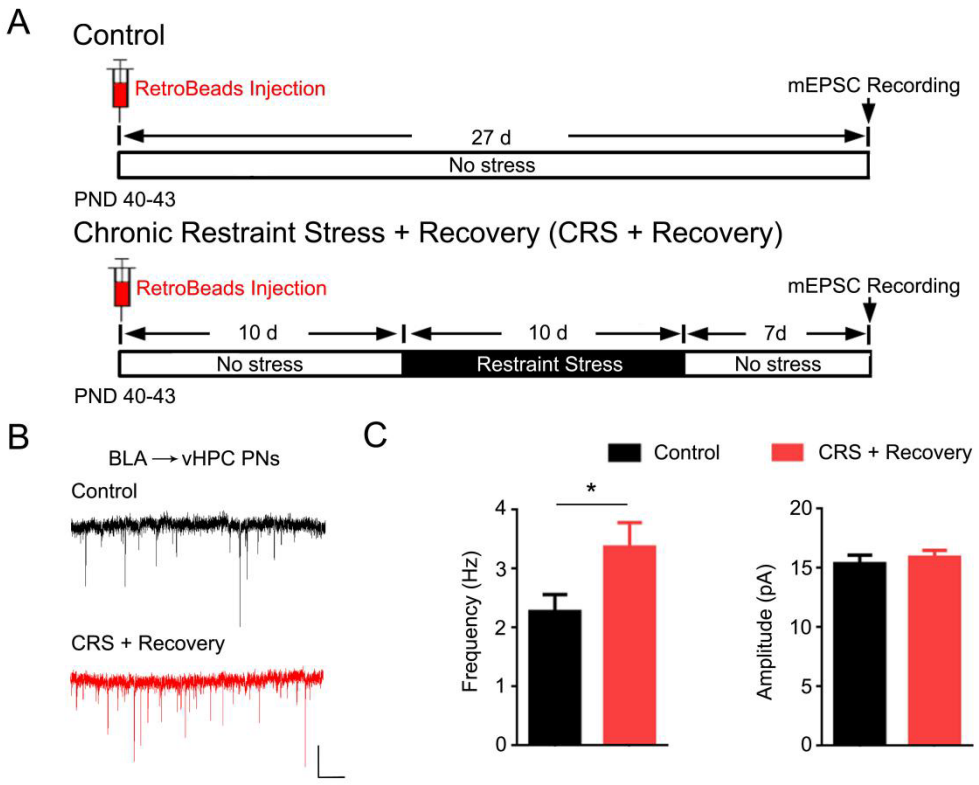

Figure S6. **The increased mEPSCs frequency in BLA→vHPC PNs by CRS persists after one week stress-free recovery.**

(A) Schematic showing the experimental design.

(B) Representative traces showing mEPSCs in BLA→vHPV PNs. Scale bar = 1 sec, 10 pA.

(C) Average mEPSCs frequency and amplitude in BLA→vHPC PNs. n=10 neurons/4 controls and n=9 neurons/4 CRS. t test for mEPSCs frequency, p=0.043; for mEPSCs amplitude, p=0.573.

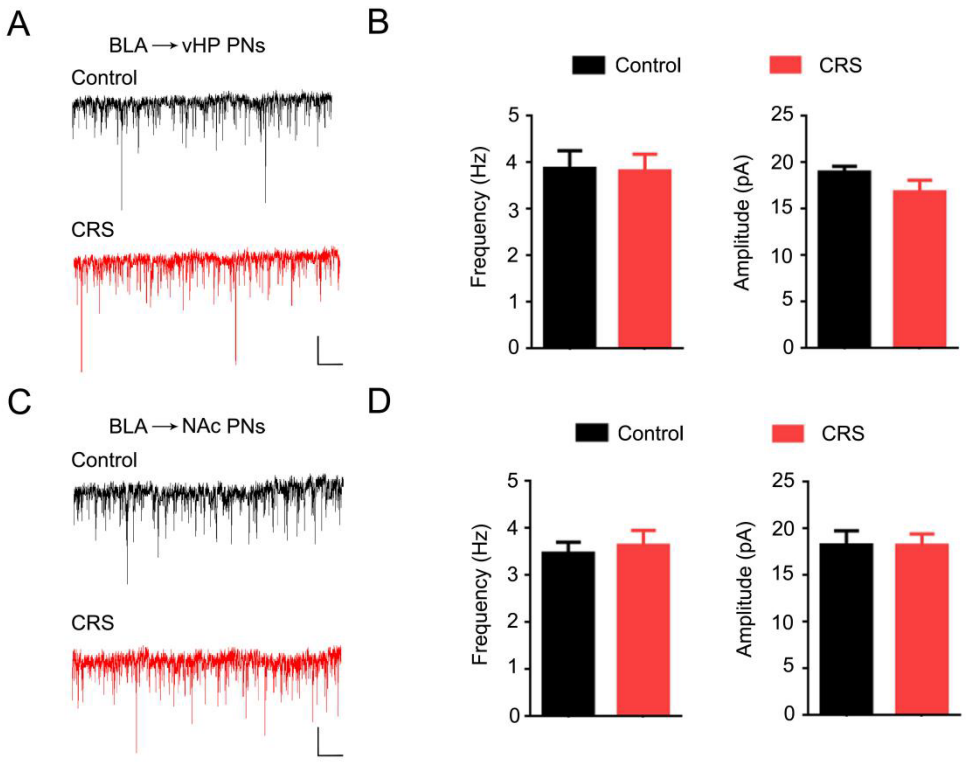

Figure S7. CRS does not affect mIPSCs in BLA→vHPC and BLA→NAc PNs.

(A) Representative traces showing mIPSCs in BLA→vHPC PNs. Scale bar = 1 sec, 10 pA.

(B) Average mIPSC frequency and amplitude in BLA→vHPC PNs. n= 10 neurons/4 controls and n= 9 neurons/4 CRS. t test for mEPSCs frequency, p=0.917; for mEPSCs amplitude, p=0.439.

(C) Representative traces showing mIPSCs in BLA→NAc PNs. Scale bar = 1 sec, 10 pA.

(D) Average mIPSC frequency and amplitude in BLA→NAc PNs. n= 11 neurons/4 controls and n= 12 neurons/4 CRS. t test for mEPSCs frequency, p=0.677; for mEPSCs amplitude, p=0.952.

Supplemental Reference

1. Liu ZP, *et al.* (2014): Chronic stress impairs GABAergic control of amygdala through suppressing the tonic GABAA receptor currents. Molecular brain 7:32.